Available online at www.sciencedirect.com

SciVerse ScienceDirect

Ceramics International 39 (2013) 5795–5803

CERAMICS INTERNATIONAL

www.elsevier.com/locate/ceramint

Influence of TiO_2 buffer layer and post-annealing on the quality of Ti-doped ZnO thin films

Y.C. Lin[a], C.Y. Hsu[b], S.K. Hung[a], D.C. Wen[c,*]

[a]Department of Mechanical Engineering, National Chiao Tung University, Taiwan, ROC
[b]Department of Mechanical Engineering, Lunghwa University of Science and Technology, Taiwan, ROC
[c]Department of Mechanical Engineering, China University of Science and Technology, Taiwan, ROC

Received 7 November 2012; received in revised form 17 December 2012; accepted 29 December 2012
Available online 11 January 2013

Abstract

Ti-doped ZnO (TZO) thin films were grown on soda lime glass (SLG) substrate without and with a TiO_2 buffer layer by radio frequency magnetron sputtering and then annealed under vacuum at 450 and 500 °C for 20 min. The structural, electrical, and optical properties of TZO films were investigated. XRD analysis shows that all TZO films are highly textured along the *c*-axis and perpendicular to the substrate. The structural properties of TZO films are improved by controlling the annealing temperature and inserting a TiO_2 buffer layer. When the films were annealed at 450 °C, the crystallinity increased, but it then decreased slightly with increase in annealing temperature from 450 to 500 °C. Due to superior crystallinity, TZO films annealed at 450 °C exhibited lower resistivity and higher average transmittances in the visible region. The improvements in crystallinity, resistivity and transmittance are more obvious when a TiO_2 buffer layer was inserted. The decrease in resistivity is mainly attributed to an increase in Hall mobility rather than carrier concentration. When the TZO films deposited on bare SLG substrate, the energy band gaps was decreased after annealing at 450 and 500 °C due to the decrease in carrier concentration. However, the absorption edge of TZO films deposited on TiO_2-buffered substrate was blue shifted, and the energy band gap was increased due to the increase of carrier concentration. In this study, the TZO film with optimal properties was grown on the TiO_2-buffered substrate and post annealed at 450 °C, achieving a resistivity of 3.76×10^{-3} Ω-cm and an average transmittance above 85%. Therefore, it can be concluded that inserting a buffer layer at an early stage of film deposition to improve crystallinity can help achieve low resistivity, high transmittance, and high energy band gap in transparent conducting TZO thin films.

Keywords: C. Optical properties; Ti-doped zinc oxide; Buffer layer; Annealing

1. Introduction

Transparent conducting oxide (TCO) films with optical transmission above 80% in the visible region and resistivity below 10^{-3} Ω-cm are extensively used in solar cells, flat panels, and light emitting diodes as well as flexible displays [1–3]. Materials such as indium tin oxide (ITO) and zinc oxide (ZnO) films are well-known transparent conductive films. Doped ZnO films are promising alternative of ITO films due to their stable electrical and optical properties. Among the various types of doped ZnO films, Ti-doped ZnO (TZO) films, in comparison with ZnO films doped with Group III elements, have more than one charge valence state. Ti^{4+} has a radius of 0.68 Å, which is smaller than that of Zn^{2+}, 0.74 Å. When titanium atoms are doped into a ZnO lattice, they act as donors by providing two free electrons, thus increasing the free carrier concentration and decreasing the resistivity. Furthermore, ZnO films doped with Ti have larger preferential *c*-axis orientation and better optical properties than pure ZnO films [4]. TCO thin films have been prepared by several techniques, including magnetron sputtering [5], chemical vapor deposition [6], and sol–gel process [7]. Among these methods, sputtering has advantages of good uniformity, high process controllability, and large-area deposition.

Recent research has studied and reported the properties of deposited TZO films. Chung et al. [8] indicated that the

*Corresponding author. Tel.: +886 2 2786 7048; fax: +886 2 2786 7253.
E-mail address: dcwen@cc.cust.edu.tw (D.C. Wen).

0272-8842/$ - see front matter © 2013 Elsevier Ltd and Techna Group S.r.l. All rights reserved.
http://dx.doi.org/10.1016/j.ceramint.2012.12.099

crystallinity of TZO films was improved with a low working pressure and a high substrate temperature, and the lowest film resistivity was obtained with 1.34 wt% of Ti added. Lu et al. [9,10] and Lin et al. [11] have reported using simultaneous magnetron co-sputtering technique to deposit TZO films. The surface roughness of TZO films increased with higher power applied to the Ti target. Wang et al. [12] investigated the effects of substrate temperature on properties of TZO films and found enhancement in TZO film properties when the substrate temperature increased from room temperature to 300 °C. Chang et al. [13] and Jiang et al. [14] studied the effects of annealing treatment on properties of TZO thin films. They reported that the film resistivity decreased and the average optical transmittance in the visible wavelength range changed slightly after annealing treatment. It is well known that TCO epitaxial thin films must be grown with low defect densities and more n-type characteristics [15]. Unfortunately, direct growth of TCO epitaxial thin film deposited on glass substrate is difficult at low growth temperature and high doping concentration due to large lattice mismatch and thermal expansion coefficient between the films and the substrates [16,17]. Several research groups have studied the growth of epitaxial Al- or Ga-doped ZnO (AZO and GZO) thin films by introducing buffer layers like Al, ZnO and SiO_2 to overcome these difficulties [18–20]. However, the effects of inserting a buffer layer on properties of TZO thin films have rarely been reported so far.

In this study, TiO_2 film was chosen as a buffer layer since titanium has high chemical resistance, high melting point, and the same hexagonal-close-packed (HCP) structure as ZnO has [21]. TZO films were deposited on TiO_2-buffered and bare soda lime glass (SLG) substrates using radio frequency (RF) magnetron sputtering and then annealed under vacuum. The structural, electrical, and optical properties of TZO films were investigated.

2. Experimental

TZO transparent conducting films and TiO_2 buffer layer were deposited on $25 \times 25 \times 1.1\ mm^3$ SLG substrates by magnetron sputtering system. The diameter of the TZO and TiO_2 targets was 50.8 mm and their thickness was 3 mm. Before deposition, the targets were pre-sputtered for 5 min to remove any contamination. The substrates were ultrasonically cleaned with acetone and de-ionized water, and then blown dry with nitrogen gas. All samples were deposited with substrate rotation in order to have a good surface morphology. The RF sputtering conditions are shown in Table 1. According to these sputtering conditions the thickness of the TZO films was ~330 nm.

Our previous study has shown that the optimal thickness of the buffer layer for AZO films with high transmittance was about 10 nm [22]. Therefore, the deposition time of TiO_2 buffer layer was adjusted to make sure that the thickness of the layer was ~10 nm. Research has found that the resistivity of TZO and AZO was improved after a vacuum post-annealing at temperatures ranging from 400 °C to 500 °C but was decreased under annealing at 600 °C [14,23]. Hence, the as-deposited samples were subsequently annealed in a tube furnace evacuated to a primary vacuum level (5.0×10^{-6} Torr) at 450 °C and 500 °C for 20 min. Moreover, another set of samples were deposited on silicon substrate for the transmission electronic microscopy (TEM) measurement.

After deposition and annealing, the surface morphological properties were analyzed using an atomic force microscope (AFM, SPA-400) and field emission scanning electron microscopy (SEM, JEOL, JSM-6500 F). The crystallographic properties of the films were determined by X-ray diffraction (Rigaku-2000 X-ray diffractometer), with Cu-Kα radiation (40 kV, 30 mA and $\lambda = 0.1541$ nm) and an angle incidence of 1°. Electrical resistivity was measured by the four-point probe method (Mitsubishi chemical MCP-T600). Carrier concentration and Hall mobility were obtained from Hall-effect measurement by the Van der Pauw method (Ecopia, HMS-3000). Optical transmittance was measured by a UV/vis/IR spectrophotometer (Jasco, V-570) in the wavelength ranging from 300 to 800 nm. All measurements were performed at room temperature in air.

3. Results and discussion

3.1. Structural properties

Fig. 1 shows the XRD patterns of TZO films prepared without and with a TiO_2 buffer layer as a function of

Table 1
Deposition parameters of TZO film and TiO_2 buffer layer.

Parameters	TZO film	TiO_2 buffer layer
Target	98 wt% ZnO, 2 wt% TiO_2 (99.995% purity)	TiO_2 (99.995%, purity)
Sputtering power	130 W, 13.56 MHz	100 W, 13.56 MHz
Base pressure	5.0×10^{-6} Torr	5.0×10^{-6} Torr
Working gas	Argon (99.995%)	Argon (99.995%)
Deposition pressure	15×10^{-3} Torr	15×10^{-3} Torr
Substrate-to-target distance	85 mm	85 mm
Substrate temperature	300 °C	100 °C
Substrate rotate vertical axis	10 rpm	10 rpm
Deposition time	70 min	–

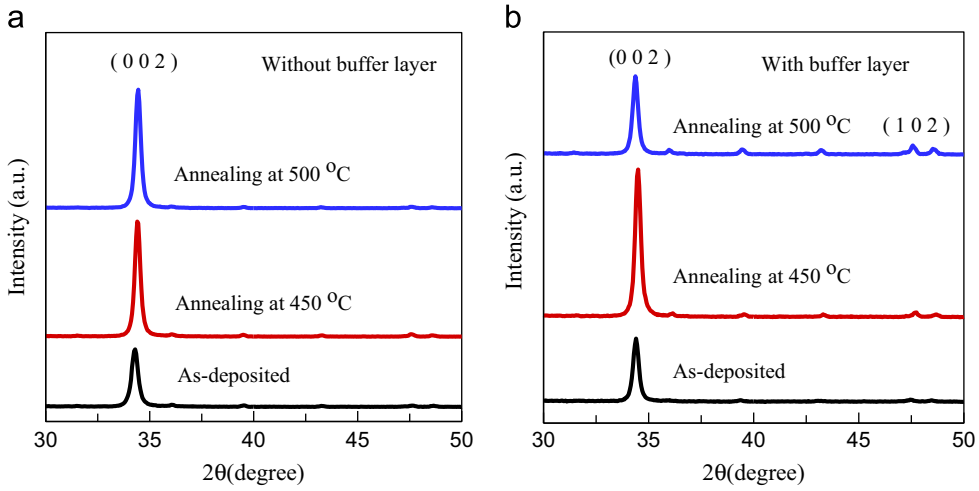

Fig. 1. XRD patterns of TZO films prepared (a) without and (b) with TiO_2 buffer layer.

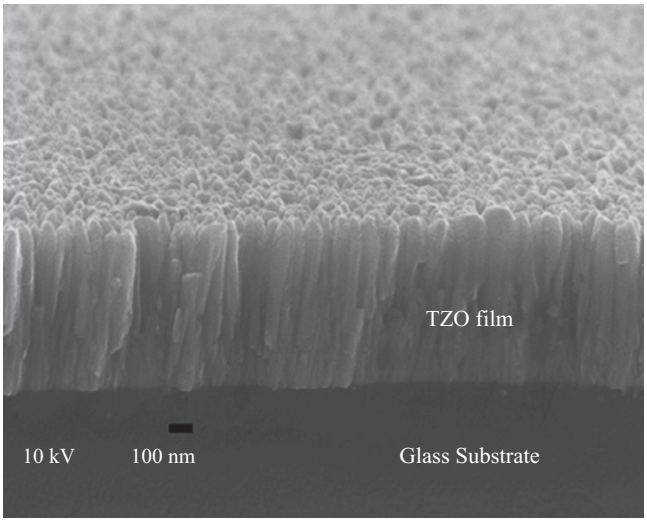

Fig. 2. SEM micrograph cross-section of as-deposed TZO film prepared without TiO_2 buffer layer.

annealing temperature. As can be seen, all films exhibited a significant (002) peak at 2θ value of 34–35°, indicating that the TZO films prepared by RF magnetron sputtering had a hexagonal wurtzite structure and showed a good *c*-axis orientation perpendicular to the substrate [24]. Fig. 2 shows SEM micrograph of cross-section of as-deposed TZO film prepared without TiO_2 buffer layer. The cross-section shows the film to have a dense columnar structure which is perpendicular to the glass substrate. This result is similar to findings previously reported [9–13]. In addition, there was no TiO_2 phase found from the XRD spectra, implying that titanium may replace zinc in the hexagonal lattice or segregate to the non-crystalline region in grain boundaries. The relative intensity of the (002) diffraction peak increased when the films were annealed at 450 °C, indicating stronger *c*-axis orientation than that of the as-deposited TZO films. The smaller intensity for the (002) diffraction peak of TZO film grown on TiO_2-buffered glass and annealed at 500 °C in comparison to that annealed at 450 °C is attributed to film deterioration (Fig. 1b). This result indicates that preferred orientation changes for a few grains in the film and the structure of TZO film is becoming more random. Thus, various grains with (002) and (102) preferred orientations normal to substrate were observed.

Lin et al. [11] mentioned that more Ti atoms substituted into Zn sites led to more compressive stress in the lattice of TZO films in a direction parallel to the surface due to an increase in substrate temperature, which could affect the lattice spacing perpendicular to the surface and cause the position of the (002) peak to shift to a lower diffraction angle than that of the ZnO bulk position (~34.45°). On the contrary, during the annealing treatment, the atoms receive energy and migrate to relative equilibrium positions, which induces a series of effects; for example, reducing the lattice strain, showing a more perfect crystallite, weakening grain boundary scattering and increasing the number of current carriers [25]. Han et al. [26] indicated that the strain of the as-grown AZO film decreased when the film was annealed due to the relaxation of planes. The (002) peak position of non-buffered TZO films was changed and shifted to the normal peak of the ZnO bulk position by annealing, as shown in Fig. 3. However, the influence of annealing on the position of the (002) peak for the films prepared with a TiO_2 buffer layer is quite distinct. It seems that TZO film deposited directly on glass is more sensitive to annealing treatment. It is supposed that the defects, induced by the lattice mismatch and thermal expansion coefficient, can get thermal energy from annealing treatment and move to the film surface, therefore, the strain in film is effectively relaxed. However, buffer layer in TZO films can preclude this kind of movement and confine most of the defects in itself. Thus the position of the (002) peak was almost unchanged.

Fig. 4 shows the full width at half-maximum (FWHM) and grain size with annealing temperature of TZO films prepared

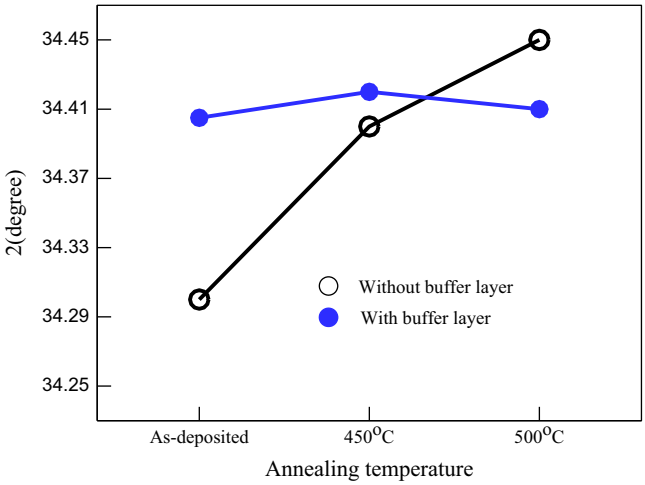

Fig. 3. Dependence of diffraction angle of (002) reflection peak on the annealing temperature.

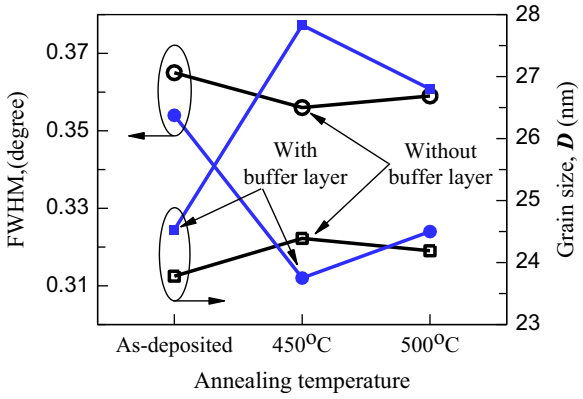

Fig. 4. FWHM and grain size as a function of annealing temperature for TZO thin films prepared without (open) and with (solid) TiO_2 buffer layer.

without and with a TiO_2 buffer layer. The grain size (D) was calculated according to Scherrer's formula:

$$D = \frac{0.9\lambda}{\beta \cos\theta} \quad (1)$$

where X-ray wave length $\lambda = 1.54$ Å, β is the FWHM, and θ is the Bragg angle of (002) peak. FWHM in all films are in range of 0.31–0.37, and grain sizes are in range of 23–28 nm. The FWHM of annealed TZO films decreased and their grain size increased as compared with the as-deposited film. The films annealed at 450 °C had larger grain size. The increase in grain size after insertion of a TiO_2 buffer layer is obvious.

Fig. 5 shows AFM images of TZO films prepared without and with a TiO_2 buffer layer and then annealed at various temperatures. Fig. 5a shows that the morphology of as-deposited films was in the shape of cobblestone and island, indicating that the growth has taken place by nucleation and coalescence during the deposition of TZO film by sputtering onto substrates. Randomly distributed nuclei may have first formed and these nuclei then grow to form observable islands. When the TZO films were annealed at 450 °C, the islands formed came closer to each other, with the larger ones appearing to grow by coalescence of smaller ones. Thus, the surface structure of films became denser and the grains grew larger, as shown in Fig. 5b. This enhancement was more obvious when a TiO_2 buffer layer was inserted. However, micro voids were observed at the grain boundaries and the surface morphology of the films became loose with open grain boundaries when the annealing temperature increased from 450 °C to 500 °C, as shown in Fig. 5c. The results confirm that the structural properties of TZO films can be improved by controlling the annealing temperature and inserting a TiO_2 buffer layer.

Surface roughness (*Ra*) was also calculated from AFM. The *Ra* value of TZO films deposited without and with a TiO_2 buffer layer is 4.224 and 5.717 nm, respectively. Relatively large *Ra* value appeared for the TZO film deposited on the TiO_2-buffered substrate. Pre-deposition of TiO_2 buffer layer increased the surface roughness of the substrate, resulted in the increase of the *Ra* value of the TZO films. *Ra* value increases when the TZO films were annealed and as the temperature increased from 450 °C to 500 °C, the surface of the TZO films became rougher. *Ra* values of the TZO films increased with increasing temperature due to the three-dimensional island growth during thermal annealing.

The bright-field TEM micrograph obtained from the cross-section of TZO film prepared with a TiO_2 buffer layer and post-annealed at 450 °C is shown in Fig. 6. The cross-section of the TZO/ TiO_2 junction reveals a good contact between the TiO_2 buffer layer and the TZO film. The thickness of the TiO_2 buffer layer is about 10 nm. The microstructure shows that the TZO film and the TiO_2 layer are both very dense and uniform. The spacing between the planes in the atomic lattice (d) of TZO film was measured by the TEM image, and the d spacing of the (002) plane was about 0.2604 nm. This value is very close to the spacing between the TZO (002) plane calculated by Bragg's law (0.2602 nm). Moreover, a grain boundary in the TZO film was clearly observed, indicating a polycrystalline structure but with a preferential orientation along the *c*-axis. With increasing annealing temperature, the polycrystallic character of TZO film became more obvious hence a low intensity of (102) peak was observed in the TZO film prepared with a TiO_2 buffer layer and then annealed at 500 °C, as shown in Fig. 1b.

3.2. Electrical properties

The resistivity (ρ), Hall mobility (μ) and carrier concentration (N) for TZO films prepared without and with a TiO_2 buffer layer as a function of annealing temperature are shown in Fig. 7. The optimal annealing temperature was 450 °C and it caused the resistivity to decrease by 30% (from 7.98×10^{-3} to 5.62×10^{-3} Ω-cm) and 45% (from 6.81×10^{-3} to 3.76×10^{-3} Ω-cm) for the films prepared without and with a TiO_2 buffer layer, respectively.

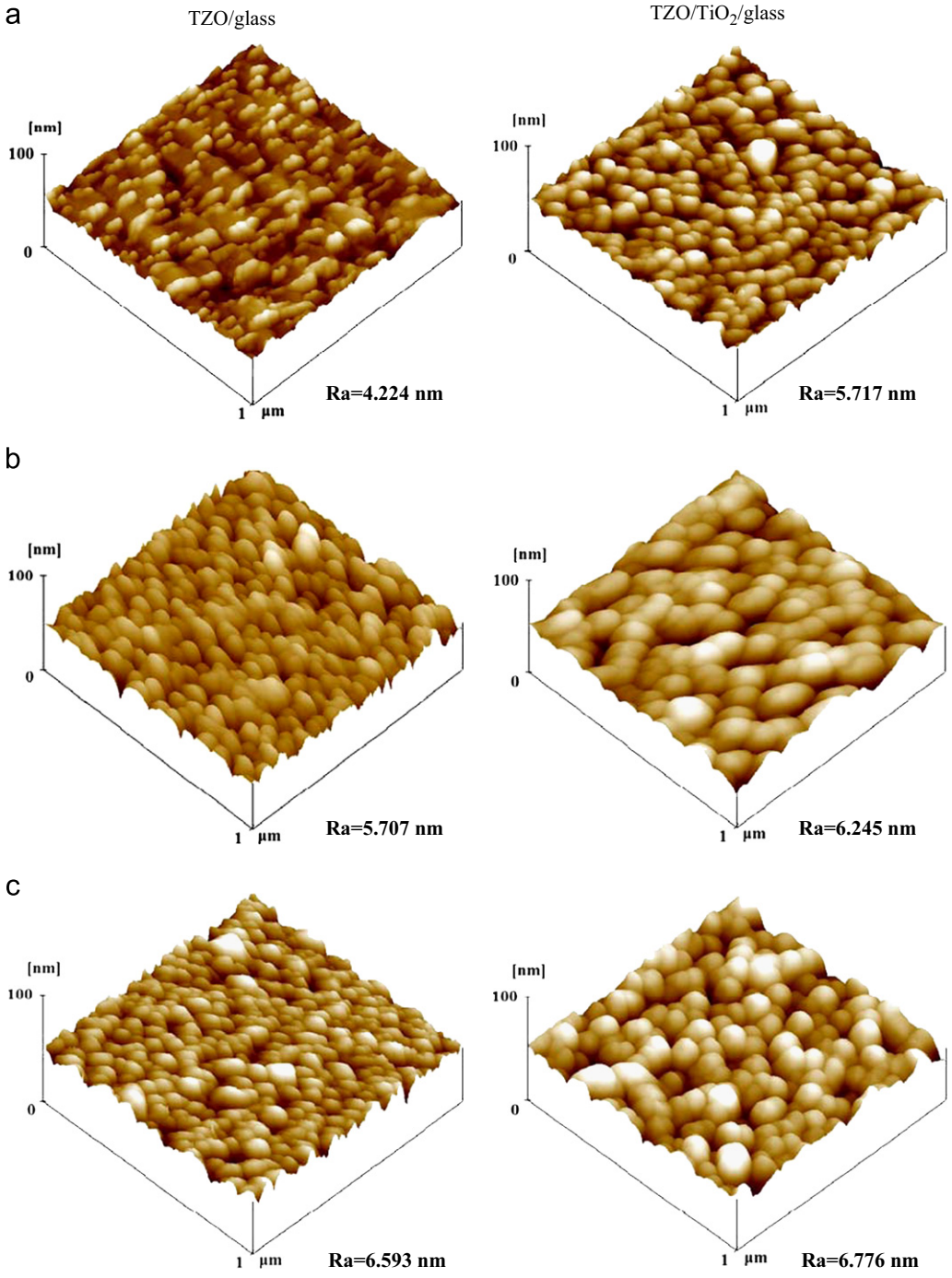

Fig. 5. AFM micrographs of TZO films prepared without (left) and with (right) TiO_2 buffer layer for the (a) as-deposited and for those annealed at (b) 450 °C and (c) 500 °C.

However, with increase in annealing temperature to 500 °C, resistivity increased.

Resistivity is a combined result of both Hall mobility and carrier concentration according to the formula of resistivity,

$$\rho = \frac{1}{Ne\mu} \tag{2}$$

where e is the electron charge. For films deposited with a TiO_2 buffer layer, the diffusion of Na atoms from SLG substrate into film could be suppressed by the buffer layer. As the TZO film annealed at 450 °C, the grain size increases. A larger grain size reduces the grain boundary scattering and increases the carrier lifetime, which results in an increase in conductivity, due to an increase in Hall mobility and carrier concentration. As a result, the sheet resistance of the TZO films decreases. In the case of annealing at 500 °C, the film became looser with open grain boundaries and grain size reduced. It implies an increase in the number of grain boundary defects and hence decreases the carrier concentration [27]. Although TiO_2 buffer layer could prevent the diffusion of Na atoms into film,

if annealing temperature is high, some Na atoms could be still diffused into TZO film through the TiO_2 layer. If Na atom substitutes zinc atom, it will become acceptor, resulting in decrease of carrier concentration [28]. Another possible reason is related to segregation of metal atoms into grain boundaries, where they become inactive as donors [29]. Therefore, with increase in annealing temperature to 500 °C, the carrier concentration decreased resulting in increasing the resistivity.

On the other hand, for films deposited without buffer layer, Na atoms diffusion from SLG substrate into TZO films during annealing, and the grain size of the films is smaller than that of the films grown on the TiO_2-buffered substrates. Thus, TZO films prepared without buffer layer demonstrate higher resistivity, as shown in Fig. 7a.

It should be noted that the decrease in lowest resistivity obtained was mainly related to increase in Hall mobility, as shown in Fig. 7b. As evidenced from XRD and AFM microscopic analyses, TZO films prepared with a TiO_2 buffer layer exhibited superior crystallinity than thin films prepared without buffer layer. Thus, increase in Hall mobility may be attributable to decrease in carrier scattering by the defects and imperfections in polycrystalline TZO, due to improved crystallinity of the buffer layer-inserted TZO film. As described above, it can be concluded that the improvement of crystallinity at an early stage of film deposition contribute to lower resistivity in transparent conducting TZO thin films.

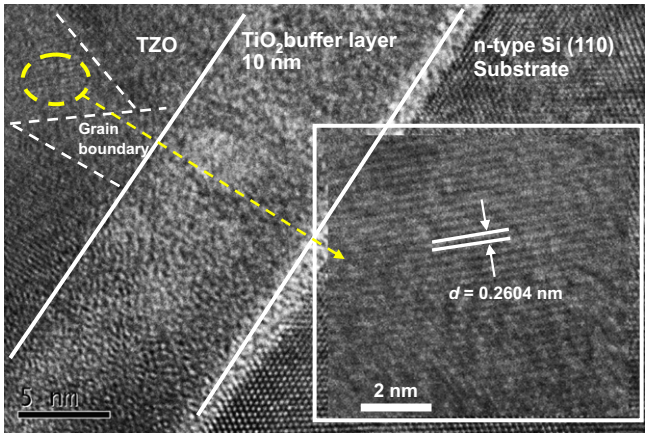

Fig. 6. Bright-field TEM micrograph of TZO film prepared with TiO_2 buffer and annealed at 450 °C.

3.3. Optical properties

Fig. 8 shows the optical transmittance spectra of TZO films prepared without and with a TiO_2 buffer layer. The average transmittances in the visible region are listed in Table 2. All films exhibited high average transmittances exceeding 83% in the visible region and enhancement in transmittance of films by annealing treatment was observed. By introducing a TiO_2 buffer layer between the SLG substrate and the TZO film, the transmittance of the as-deposited TZO film is lower than the film prepared without buffer layer. However, the transmittance was improved to 85% after annealing at 450 °C due to its superior crystallinity.

Fig. 9 plots of α^2 versus hv (where α is the absorption coefficient and hv is the photon energy). The energy band gap (E_g) can be estimated by extrapolations of the straight-line part of the plot to the photon energy axis. As shown in Fig. 8b, for TZO film deposited with a TiO_2 buffer layer and annealed at 450 °C, the absorption edge has been blue shifted compared with the as-deposited TZO film, and correspondingly, the energy band gap is increased from 3.262 to 3.345 eV (Fig. 9b), which is attributed to Burstein–Mott effect [30] due to the increase of carrier concentration by introducing a TiO_2 layer. However, when the annealing temperature increased from 450 to 500 °C, the energy band gap decreased to 3.307 eV, which is consistent with decrease in carrier concentration. In Fig. 9, the absorption coefficient α was calculated using the equation [31]:

$$\alpha = \frac{\ln 100/T}{t} \tag{3}$$

where t is film thickness and T is transmittance. The energy band gap dependence of the absorption coefficient is given

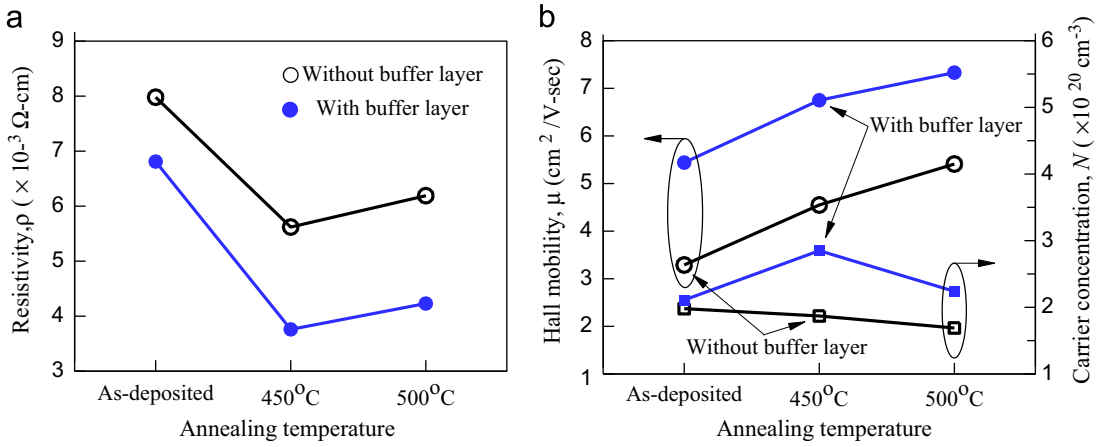

Fig. 7. (a) Resistivity and (b) Hall mobility and carrier concentration as a function of annealing temperature for TZO thin films prepared without (open) and with (solid) TiO_2 buffer layer.

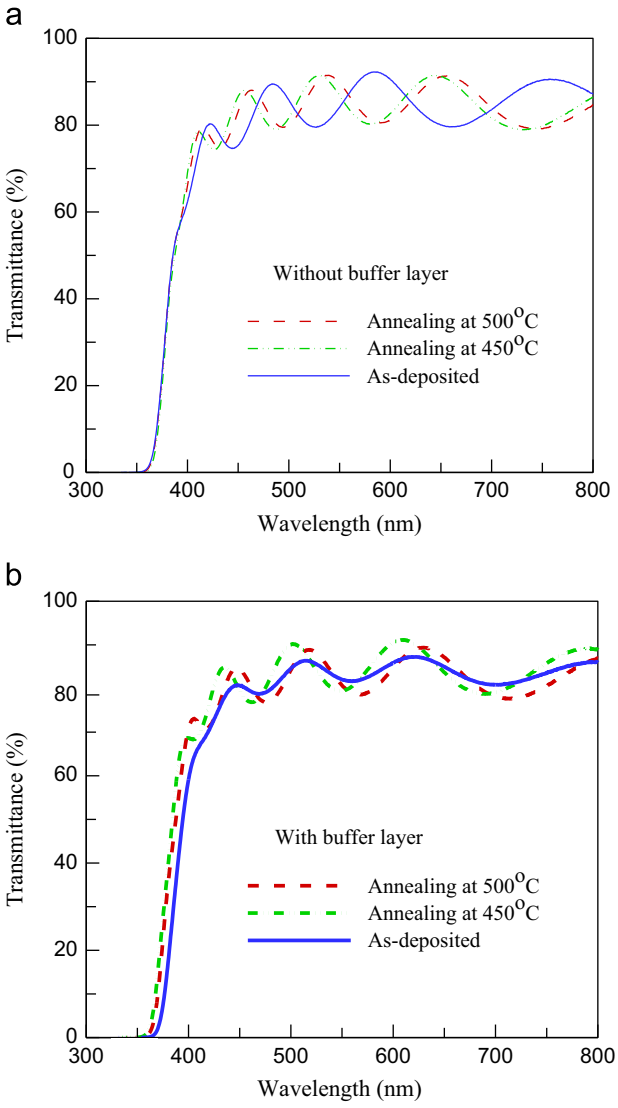

Fig. 8. Optical transmittance spectra of TZO films prepared (a) without and (b) with TiO_2 buffer layer.

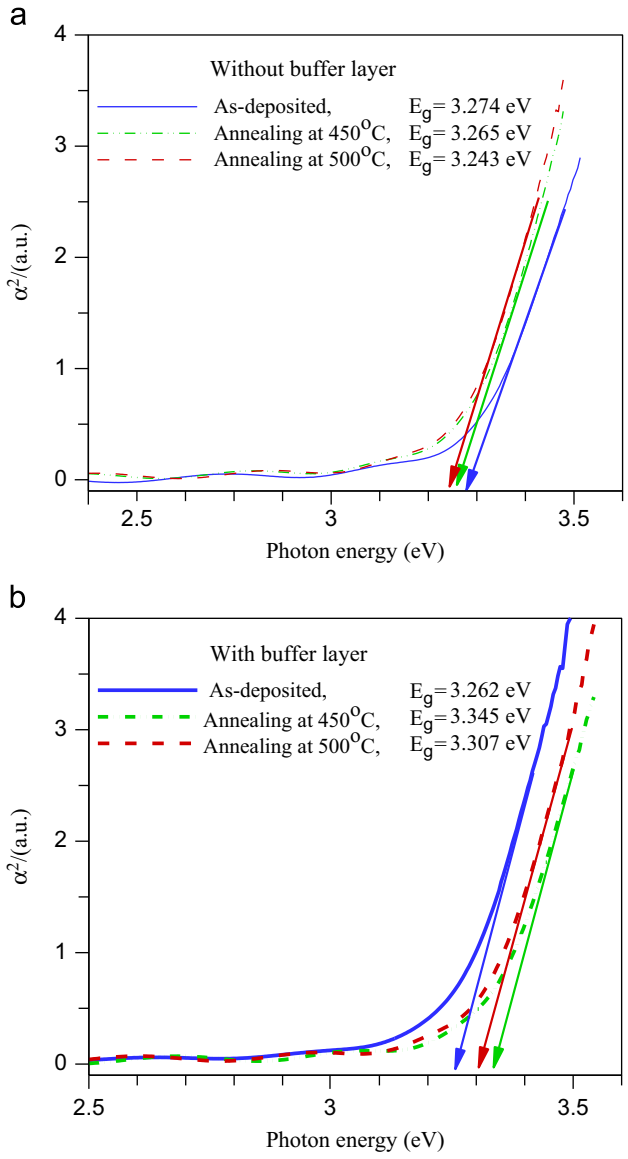

Fig. 9. Plots of α^2 versus $h\nu$ for TZO films prepared (a) without and (b) with TiO_2buffer layer.

Table 2
Average optical transmittances of TZO films in the visible region (%).

Sample	As-deposited	Annealed at 450 °C	Annealed at 500 °C
Without buffer layer	84.86	85.25	85.11
With buffer layer	83.65	85.17	84.21

by the equation [32]:

$$(\alpha h\nu)^2 = A(h\nu E_g) \quad (4)$$

where A is constant. As can be seen in Table 2 and Fig. 7b, for the TiO_2 buffered TZO films, the variation trend of average transmittance and carrier concentration is agree with each other. Therefore, when the carrier concentration decreases or increases the energy band gap also decreases or increases.

For TZO films deposited without buffer layer, the absorption edges do not depend on variety of annealing temperature and are almost same (Fig. 8a). However, the energy band gap was decreased from 3.274 eV to 3.265 and 3.243 eV for the films annealed at 450 and 500 °C compared with the case of as-deposited TZO film (Fig. 9a) since the carrier concentration was decreased due to the diffusion of Na atoms into the TZO films (Fig. 7b).

4. Conclusions

TZO films were prepared on TiO_2-buffered and non-buffered glass substrates by RF sputtering and followed by annealing under vacuum at 450 °C and 500 °C for 20 min. The electrical and optical properties of TZO films were strongly dependent on film crystallinity. The structural

properties of TZO films were highly textured along the *c*-axis and perpendicular to the substrate and could be improved by controlling the annealing temperature and inserting a TiO_2 buffer layer. TZO film prepared without buffer layer and annealed at 450 °C exhibited lower resistivity and higher average transmittances in the visible region due to its superior crystallinity. These properties were further improved by inserting a TiO_2 buffer layer, and a resistivity of 3.76×10^{-3} Ω-cm and an average transmittance more than 85% were achieved. The decrease in resistivity was mainly attributed to increase in Hall mobility rather than carrier concentration. When the TZO films deposited on bare SLG substrate, the energy band gap was decreased after annealing at 450 and 500 °C due to the decrease in carrier concentration. However, the absorption edge of TZO films deposited with a TiO_2 buffer layer was blue shifted, and the energy band gap was increased due to the increase of carrier concentration. The results indicate that inserting a buffer layer at an early stage of film deposition to improve crystallinity helps obtain lower resistivity, higher transmittance, and higher energy band gap in transparent conducting TZO thin films.

References

[1] D.Y. Ku, I.H. Kim, I. Lee, K.S. Lee, T.S. Lee, J.H. Jeong, B. Cheong, Y.J. Baik, W.M. Kim, Structural and electrical properties of sputtered indium–zinc oxide thin films, Thin Solid Films 515 (2006) 1364–1369.

[2] J. Lee, J. Metson, P.J. Evans, R. Kinsey, D. Bhattacharyya, Implanted ZnO thin films: microstructure, electrical and electronic properties, Applied Surface Science 253 (2007) 4317–4321.

[3] R. Das, T. Jana, S. Ray, Degradation studies of transparent conducting oxide: a substrate for microcrystalline silicon thin film solar cells, Solar Energy Materials and Solar Cells 86 (2005) 207–216.

[4] S. Singh, N. Rama, K. Sethupathi, M.S. Ramachandra Rao, Correlation between electrical transport, optical, and magnetic properties of transition metal ion doped ZnO, Journal of Applied Physics 103 (2008) 07D108 (3p.).

[5] S.S. Lin, J.L. Huang, D.F. Lii, Effect of substrate temperature on the properties of Ti-doped ZnO films by simultaneous RF and DC magnetron sputtering, Materials Chemistry and Physics 90 (2005) 22–30.

[6] K. Zheng, L. Gu, D. Sun, X.L. Mo, G. Chen, The properties of ethanol gas sensor based on Ti doped ZnO nanotetrapods, Materials Science and Engineering: B 166 (2009) 104–107.

[7] C.Y. Tsay, H.C. Cheng, C.Y. Chen, K.J. Yang, C.K. Lin, The properties of transparent semiconductor $Zn_{1-x}Ti_xO$ thin films prepared by the sol–gel method, Thin Solid Films 518 (2009) 1603–1606.

[8] J.L. Chung, J.C. Chen, C.J. Tseng, The influence of titanium on the properties of zinc oxide films deposited by radio frequency magnetron sputtering, Applied Surface Science 254 (2008) 2615–2620.

[9] Y.M. Lu, C.M. Chang, S.I. Tsai, T.S. Wey, Improving the conductance of ZnO thin films by doping with Ti, Thin Solid Films 447–448 (2004) 56–60.

[10] J.J. Lu, Y.M. Lu, S.I. Tasi, T.L. Hsiung, H.P. Wang, L.Y. Jang, Conductivity enhancement and semiconductor–metal transition in Ti-doped ZnO films, Optical Materials 29 (2007) 1548–1552.

[11] S.S. Lin, J.L. Huang, P. Šajgalik, The properties of Ti-doped ZnO films deposited by simultaneous RF and DC magnetron sputtering, Surface and Coatings Technology 191 (2005) 286–292.

[12] F.H. Wang, H.P. Chang, J.C. Chao, Improved properties of Ti-doped ZnO thin films by hydrogen plasma treatment, Thin Solid Films 519 (2011) 5178–5182.

[13] H.P. Chang, F.H. Wang, J.C. Chao, C.C. Huang, H.W. Liu, Effects of thickness and annealing on the properties of Ti-doped ZnO films by radio frequency magnetron sputtering, Current Applied Physics 11 (2011) S185–S190.

[14] M. Jiang, X. Liu, G. Chen, J. Cheng, X. Zhou, Preparation and photoelectric properties of Ti doped ZnO thin films, Journal of Materials Science: Materials in Electronics 20 (2009) 1225–1228.

[15] M. Snure, A. Tiwari, Structural, electrical, and optical characterizations of epitaxial $Zn_{1-x}Ga_xO$ films grown on sapphire (0001) substrate, Journal of Applied Physics 101 (2007) 124912 (6 pages).

[16] S.W. Shin, Y.B. Kwon, A.V. Moholkar, G.S. Heo, I.O. Jung, J.H. Moon, J.H. Kim, J.Y. Lee, Hydrothermally grown ZnO buffer layer for the growth of highly (4 wt%) Ga-doped ZnO epitaxial thin films on $MgAl_2O_4$ (111) substrates, Journal of Crystal Growth 322 (2011) 45–50.

[17] K.H. Bang, D.K. Hwang, J.M. Myoung, Effects of ZnO buffer layer thickness on properties of ZnO thin films deposited by radio-frequency magnetron sputtering, Applied Surface Science 207 (2003) 359–364.

[18] B.T. Lee, T.H. Kim, S.H. Heong, Growth and characterization of single crystalline Ga-doped ZnO films using RF magnetron sputtering, Journal of Physics D 39 (2006) 957–961.

[19] C.Y. Hsu, C.H. Tsang, Effects of ZnO buffer layer on the optoelectronic performances of GZO films, Solar Energy Materials and Solar Cells 92 (2008) 530–536.

[20] K.H. Ri, Y.B. Wang, W.L. Zhou, J.X. Gao, X.J. Wang, J. Yu, The effect of SiO_2 buffer layer on the electrical and structural properties of Al-doped ZnO films deposited on soda lime glasses, Applied Surface Science 257 (2011) 5471–5475.

[21] F. Li, D. Li, J. Dai, H. Su, L. Wang, Y. Pu, W. Fang, F. Jiang, Effect of the initial thin Ti buffer layers on the quality of ZnO thin films grown on Si(111) substrates by MOCVD, Superlattices and Microstructures 40 (2006) 56–63.

[22] J.Y. Kao, C.Y. Hsu, G.C. Chen, D.C. Wen, The characteristics of transparent conducting Al-doped zinc oxide thin films deposited on polymer substrates, Journal of Materials Science: Materials in Electronics 23 (2012) 1352–1360.

[23] C.Y. Hsu, Y.C. Lin, L.M. Kao, Y.C. Lin, Effect of deposition parameters and annealing temperature on the structure and properties of Al-doped ZnO thin films, Materials Chemistry and Physics 124 (2010) 330–335.

[24] M.L. Cui, X.M. Wu, L.J. Zhuge, Y.D. Meng, Effects of annealing temperature on the structure and photoluminescence properties of ZnO films, Vacuum 81 (2007) 899–903.

[25] H.T. Cao, Z.L. Pei, J. Gong, C. Sun, R.F. Huang, L.S. Wen, Transparent conductive Al and Mn doped ZnO thin films prepared by DC reactive magnetron sputtering, Surface and Coatings Technology 184 (2004) 84–92.

[26] J.H. Han, Y.S. No, T.W. Kim, J.Y. Lee, J.Y. Kim, W.K. Choi, Microstructural and surface property variations due to the amorphous region formed by thermal annealing in Al-doped ZnO thin films grown on n-Si (100) substrates, Applied Surface Science 256 (2010) 1920–1924.

[27] W. Liu, G. Du, Y. Sun, Y. Xu, T. Yang, X. Wang, Y. Chang, F. Qiu, Al-doped ZnO thin films deposited by reactive frequency magnetron sputtering: H_2-induced property changes, Thin Solid Films 515 (2007) 3057–3060.

[28] X.D. Zhang, H.B. Fan, J. Sun, Y. Zhao, Effect of substrates on the properties of p-type ZnO films, Physica E 39 (2007) 267–270.

[29] C. Guillen, J. Herrero, Optical, electrical and structural characteristics of Al:ZnO thin films with various thicknesses deposited by DC sputtering at room temperature and annealed in air or vacuum, Vacuum 84 (2010) 924–929.

[30] K.H. Kim, K.C. Park, D.Y. Ma, Structural, electrical and optical properties of aluminum doped zinc oxide films prepared by radio frequency magnetron sputtering, Journal of Applied Physics 81 (1997) 7764–7772.
[31] R. Swanepoel, Determination of the thickness and optical constants of amorphous silicon, Journal of Physics E: Scientific Instruments 16 (1983) 1214–1222.
[32] V.R. Shinde, T.P. Gujar, C.D. Lokhande, R.S. Mane, S.H. Han, Mn doped and undoped ZnO films: a comparative structural, optical and electrical properties study, Materials Chemistry and Physics 96 (2006) 326–330.